The Journal of Chemical Physics

Iron phthalocyanine on Cu(111): Coverage-dependent assembly and symmetry breaking, temperature-induced homocoupling, and modification of the adsorbate-surface interaction by annealing

Cite as: J. Chem. Phys. **144**, 094702 (2016); https://doi.org/10.1063/1.4942121
Submitted: 30 November 2015 • Accepted: 02 February 2016 • Published Online: 01 March 2016

Olesia Snezhkova, Felix Bischoff, Yuanqin He, et al.

Iron phthalocyanine on Cu(111): Coverage-dependent assembly and symmetry breaking, temperature-induced homocoupling, and modification of the adsorbate-surface interaction by annealing

Olesia Snezhkova,[1] Felix Bischoff,[2] Yuanqin He,[2] Alissa Wiengarten,[2] Shilpi Chaudhary,[1] Niclas Johansson,[1] Karina Schulte,[3] Jan Knudsen,[1,3] Johannes V. Barth,[2] Knud Seufert,[2,a)] Willi Auwärter,[2] and Joachim Schnadt[1]

[1]*Division of Synchrotron Radiation Research, Department of Physics, Lund University, P.O. Box 118, 221 00 Lund, Sweden*

[2]*Physik Department E20, Technische Universität München, James-Franck-Straße 1, 85748 Garching, Germany*

[3]*MAX IV Laboratory, Lund University, P.O. Box 118, 221 00 Lund, Sweden*

(Received 30 November 2015; accepted 2 February 2016; published online 1 March 2016)

We have examined the geometric and electronic structures of iron phthalocyanine assemblies on a Cu(111) surface at different sub- to mono-layer coverages and the changes induced by thermal annealing at temperatures between 250 and 320 °C by scanning tunneling microscopy, x-ray photoelectron spectroscopy, and x-ray absorption spectroscopy. The symmetry breaking observed in scanning tunneling microscopy images is found to be coverage dependent and to persist upon annealing. Further, we find that annealing to temperatures between 300 and 320 °C leads to both desorption of iron phthalocyanine molecules from the surface and their agglomeration. We see clear evidence of temperature-induced homocoupling reactions of the iron phthalocyanine molecules following dehydrogenation of their isoindole rings, similar to what has been observed for related tetrapyrroles on transition metal surfaces. Finally, spectroscopy indicates a modified substrate-adsorbate interaction upon annealing with a shortened bond distance. This finding could potentially explain a changed reactivity of Cu-supported iron phthalocyanine in comparison to that of the pristine compound. [http://dx.doi.org/10.1063/1.4942121]

I. INTRODUCTION

Metal phthalocyanines (MPcs) have considerable potential for the use in new functional nanoscale materials due to the possibility of accurate characterization and manipulation of their chemical state. Moreover, MPcs exhibit excellent chemical and thermal stabilities, uncomplicated synthesis, and tunable physical properties,[1,2] and, indeed, today they are widely employed as building blocks for molecular switches[3] and for molecular[4] and quantum computing devices, e.g., for data storage.[5] These interesting properties of MPcs have spurred significant interest in the adsorption of metal phthalocyanines on single crystal surfaces of materials such as copper, silver, and aluminium.[6–9] Surface-driven modification of the molecular properties plays an important role, and recent research into phthalocyanine compounds includes the control of the Kondo effect,[10] switching of magnetic anisotropy,[11] and uneven charge transfer leading to distortion and symmetry reduction.[12]

The preparation of MPc monolayers (ML) on metal surfaces by thermal evaporation onto the room temperature surface is often tedious since it is difficult to determine the exact amount of deposited material. Moreover, non-reproducible deposition rates when using crucibles make the procedure even less reliable. Instead, the most convenient and thus widely used technique for creating a homogeneous metal-supported monolayer is to anneal a multilayer at temperatures close to the MPc's evaporation temperature.[2,13–15] However, annealing can modify the properties of the MPc when deposited on reactive surfaces.[16] For example, upon heating of a submonolayer of iron phthalocyanine (FePc) supported on a Ag(111) surface to 200 °C, topography changes are observed in scanning tunneling microscopy (STM) images, with the FePc molecules rearranging themselves in a more closely packed and well-ordered structure than after room temperature deposition.[17] Even chemical reactions can take place: both MPcs and porphine molecules, which are close structural and electronic relatives of MPcs, are dehydrogenated and undergo a homocoupling reaction on Ag(111) when the sample is heated up to a compound-specific temperature of the order of several hundred °C.[16,18] Today, similar schemes are also known from a large variety of other compounds and are being used for on-surface covalent synthesis (see, e.g., Ref. 19). Therefore, it is of interest to determine whether dehydrogenation and homocoupling also take place in the case of FePc on Cu(111), at what temperatures these changes occur, and to understand the physics of the involved surface and reaction processes.

Here, we use STM, x-ray photoelectron spectroscopy (XPS), temperature-dependent x-ray photoelectron

a)Present address: Institut für Chemie, Karl-Franzens-Universität Graz, 8010 Graz, Austria.

spectroscopy (TD-XPS), and x-ray absorption spectroscopy (XAS) to thoroughly characterize FePc layers on Cu(111) prepared at room temperature and annealed to temperatures above 300 °C. Aspects that we address are the molecular arrangements at different coverages, symmetry breaking observed in the STM images, and modification of the adsorbate structure and interaction with the Cu(111) support upon annealing. As for other metal surface-supported macrocycles, we also find for FePc/Cu(111) that annealing leads to homocoupling between adjacent adsorbates and that both polymerized and isolated molecules are put into a state of stronger surface bonding, which manifests itself as a shortened surface-adsorbate distance.

II. EXPERIMENTAL PROCEDURES

A. XPS and XAS experiments

High-resolution x-ray photoelectron spectroscopy data were recorded at beamline I311[20] on the MAX II electron storage ring of the MAX IV Laboratory in Lund, Sweden. The instrument has separate preparation and analysis chambers connected by a gate valve. The base pressure is 1×10^{-10} mbar in the preparation chamber and in the mid 10^{-11} range in the analysis chamber. The measurements were performed using a Scienta SES200 electron energy analyzer. The overall instrumental resolution used in the measurement of the C 1s core level spectra was 90 meV and 125 meV in the case of the N 1s spectra. After each core level measurement, the energy scale was calibrated to the Fermi edge. Before further analysis a background was removed from the x-ray photoelectron (XP) spectra (Shirley in the case of the C 1s and polynomial in that of the N 1s line). The XP spectra were, arbitrarily, normalized to their area after background removal.

The N 1s XAS data were recorded on the same instrument in Auger yield mode using an analyzer pass energy of 100 eV. The kinetic energy window was chosen as to map the N KVV Auger electrons at a kinetic energy of 370 eV. The x-rays were linearly polarized, with the E-field orientation either parallel (normal light incidence on the sample) or at 20° (grazing incidence) from the surface. The photon energy resolution was set to 60 meV. The energy was calibrated from a measurement of a suitable core level spectrum excited with first and second order light. The estimated error of this procedure is ±50 meV.

The sample was a Cu(111) single crystal surface aligned to <0.1° with respect to the nominal orientation. The sample was mounted on the manipulator using a tungsten wire loop. Temperature measurement was performed using a type K thermocouple spot-welded to the edge of the crystal. The surface was cleaned prior to organic film deposition by repeated sputter-annealing treatments. For sputtering 1 kV argon ions were used at a pressure of 2×10^{-7} mbar, and for annealing, the sample was kept at 525 °C for 10 min. The cleanness of the Cu(111) single crystal was verified by XPS.

FePc with purity >90%, purchased from Sigma-Aldrich, was degassed *in vacuo* by heating to 330 °C for 2 weeks and to near-sublimation temperature for 3 h just before depositing onto the Cu(111) crystal. The desired FePc coverage on the surface obtained by adapting the deposition time. A proper monolayer was created by step-by-step deposition, with the amount of molecules deposited determined from the ratio of molecule to Cu support signal; the C 1s and Cu 3p core-level spectra were recorded and their ratio was plotted versus time of deposition. The start of second-layer growth was inferred from the change in linearity of the ratio. All samples were prepared at room temperature and then gradually annealed to record the temperature-induced modification of the FePc layer at temperatures up to a maximum temperature of 520 °C.

Extended exposure of the sample to x-rays, with an exposure time of the order of several minutes, led to the occurrence of beam damage-related features in the XP spectra. The first XPS experiments were therefore aimed at identifying the rate of beam damage by monitoring the time evolution of its occurrence for a stationary sample by measuring fast consecutive XP spectra of the different core levels. From these measurements, one could then infer the maximum permissible illumination time of a single spot on the sample surface. In subsequent XPS and XAS measurements the sample was then continuously displaced during acquisition at a speed higher than that required to ensure that no portion of the surface was irradiated for a longer time than permissible.

B. STM experiments

STM was performed using a CreaTec low-temperature STM instrument mounted on a custom-designed ultrahigh vacuum chamber at the Physics Department of the Technical University of Munich. All STM images were obtained at liquid helium temperature (5 K) at a pressure below 2×10^{-10} mbar. The images were recorded in constant current mode using an electrochemically etched W tip. dI/dV maps were recorded in constant height mode. The sample was prepared using the same type of recipe as in the XPS experiments. The topography of the FePc sub- and mono-layers was imaged before and after sequential annealing to different temperatures: 250 °C for 10 min, 270 °C for 30 min, and 300 °C for 25 min. The coverages were determined using the "flooding" technique, i.e., the area featuring an apparent height above a threshold value corresponding to the molecules was measured.[21] The thus obtained coverages were normalized to the value for the single layer, which could not accommodate additional FePc adsorbates. This layer was made up of islands of different overlayer structures and densities.

For the STM experiments, FePc powder (90% dye content; Sigma Aldrich) was triple purified by thermal gradient sublimation and degased at 20 °C below its evaporation temperature for several days before use.[22]

III. RESULTS

A. Molecular orientation, binding site, and symmetry reduction in the room temperature preparation

1. Scanning tunneling microscopy

In this work, we report STM images of molecular assemblies of FePc/Cu(111) in the average coverage range

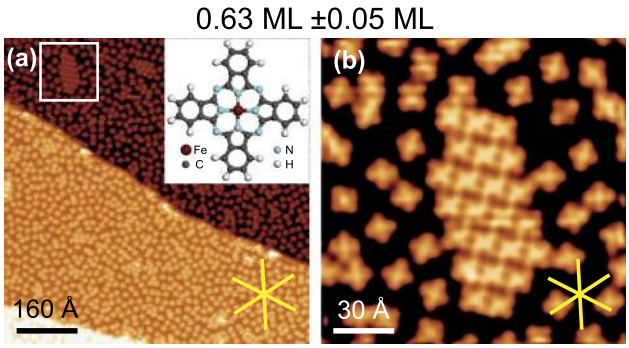

FIG. 1. STM images of 0.63 ML FePc/Cu(111). Scanning parameters: +0.75 V, 0.08 nA. (a) Larger-scale overview, 800×800 Å^2, inset: chemical structure of FePc. (b) Detailed view of the indicated area in (a), 150×150 Å^2. The close-packed directions of the Cu(111) surface are indicated by the yellow stars.

from 0.6 to 1 ML. Additional STM images not shown here were obtained at coverages below 0.6 ML and slightly above 1 ML as well as at further intermediate coverages. The findings reported here are consistent with previous STM work,[23,24] but complete them with additional data. In particular, we report on the structural parameters of several different molecular assemblies, which have not been observed previously.

In Figures 1 and 2, STM images and structures of the molecular assemblies of FePc/Cu(111) at average coverages of 0.63, 0.80, 0.98, and 1.00 ML (all ±0.05 ML) are presented. A central parameter in the discussion of the assemblies is the orientation of the FePc adsorbates. We will specify this orientation in terms of the orientation of the dihedral axes, as identified in the D_{4h} symmetry of the free molecule. We term the two dihedral axes which are parallel to opposite isoindole units as the *molecular axes* [cf. the molecular structure in the inset of Fig. 1(a)].

At the lowest coverages up to approximately 0.50 to 0.65 ML, isolated adsorbates are found on the Cu(111) surface. Only towards the upper end of this range, also islands are observed. Hence, at low coverage, the adsorbate-surface interactions dominate intermolecular interactions. The binding site of the isolated molecules, in terms of the placement of the central iron ion, is a bridge site, which we have identified from carbon monoxide co-adsorption experiments (cf. Fig. S1 in the supplementary material[25]). The isolated adsorbates are aligned with one of their molecular axes along one of the close-packed crystal directions, which in Figures 1 and 2 have been identified by yellow stars. Even in more closely packed islands observed at approximately 0.6 ML coverage, this alignment is retained, as is seen from Fig. 1. In these islands, all molecules are oriented identically, and the overlayer structure is commensurate with the Cu(111) surface. An analysis of images such as in Fig. 1(b) which contain both isolated molecules and islands provides evidence for the same bridge binding site in both cases. We also note that the bias-dependent contrast is the same for the isolated molecules and for those in the islands, lending additional support for the assertion of bridge site binding also in the islands.

At an average coverage of 0.80 ML [Figs. 2(a)-2(f)] two different molecular assemblies are observed with packing densities which are identical to within the measurement uncertainties. The first of these, shown in Figs. 2(a)-2(c), is the same as that found at 0.63 ML and features a unique orientation of the FePc adsorbates with one of the molecular axes aligned along a close-packed row. Its unit cell, displayed as a red tetragon in Figs. 2(b) and 2(c), is oblique; the lattice constants and angles are provided in the figure caption. The dimensions and shape of the unit cell are consistent with bridge site bonding, already confirmed for the 0.63 ML coverage. The other structure found at this coverage, shown in Figs. 2(d)-2(f), has a larger unit cell with differently oriented FePc adsorbates. The orientation of individual adsorbates is along the close-packed rows, but may also deviate from this direction by ±5°. The deviation is the same for all molecules in a particular island. In the STM images, one can now also discern rows of molecules which are aligned (or quasi-aligned with a deviation of up to ±5°) along a particular close-packed surface direction, while the adsorbates in the adjacent rows are aligned (or quasi-aligned) with another close-packed surface direction.

At even higher coverage, i.e., at 0.9 ML–1 ML, the FePc molecules still form a seemingly commensurate overlayer on the surface [Figs. 2(g)-2(l)]. However, new adsorbate orientations are observed. At 0.9 ML, islands are found in which the orientation of the adsorbates alternates between 5° and 12° away from the close-packed directions of the Cu(111) surface. Yet another assembly can be identified at a coverage of 1 ML [Figs. 2(j)-2(l)]. In this assembly, which has the same molecule packing density as that shown in Figs. 2(g)-2(i), all adsorbates are rotated by 12° from the close-packed surface rows. The parameters of the assembly are in agreement with those specified in the early investigation by Buchholz and Somorjai.[26] The monolayer is not completely made up from this latter structure, however; instead, different types of structures of the types displayed in Fig. 2 with different packing densities are seen to co-exist. Nevertheless, it is not possible to accommodate additional molecules in the monolayer, and further deposition of FePc molecules instead results in second-layer growth.

In comparison to the fourfold symmetry of molecules in the gas phase, a symmetry reduction can be observed in the STM images at all coverages. As is seen in Figs. 2(a) and 2(d) up to 0.8 ML coverage the observed symmetry is twofold, i.e., of the "I-type" with opposite isoindole units along one of the molecular axes appearing brighter and those along the perpendicular direction darker. In contrast, for isolated molecules at low coverage, it is the axis oriented perpendicular to the close-packed row which appears bright.[27] In the STM images obtained at an even higher coverage of 0.98 ML, other types of symmetry breaking are observed in addition to the I-type of adsorbates [Fig. 2(g)]. We classify them in terms of their appearance as T- and L-type symmetry reduction. In addition, also adsorbates of the fully symmetric type have been observed (not shown). Further, we note that at this coverage, the bright axes of the twofold symmetric I-type are oriented perpendicularly to the dense-packed Cu direction, similarly to isolated FePc molecules at low coverage.

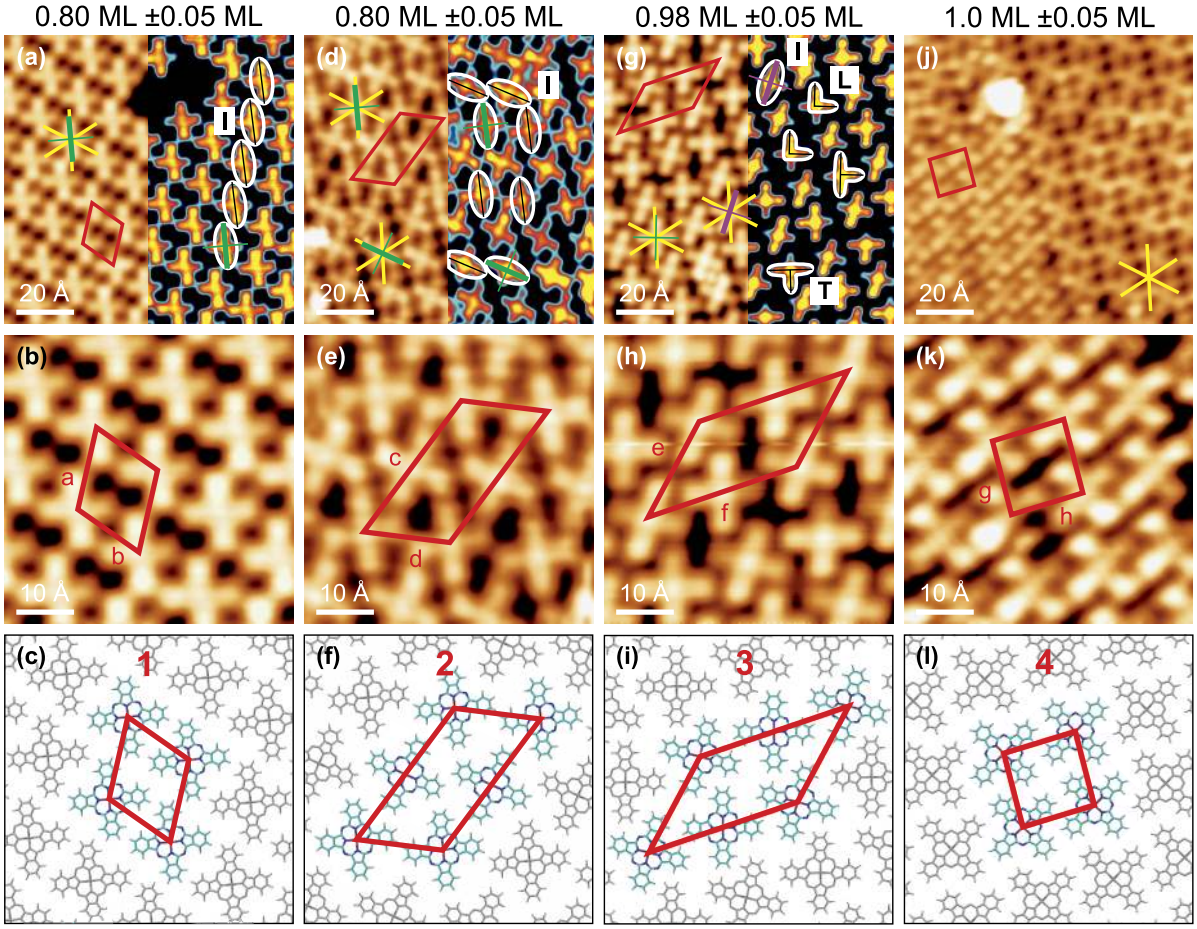

FIG. 2. STM images and schematic structures of the FePc/Cu(111) assemblies at coverages between 0.80 and 1.00 ML, illustrating the different observed molecular assemblies in this coverage range. The layers were grown at room temperature. The red tetragons depict the overlayer unit cells, while the yellow stars mark the directions of the close-packed rows of the Cu(111) surface. The image size in the top row is 100×100 Å^2, while it is 50×50 Å^2 in the middle row. ((a)-(c)) 0.80 ML coverage, +0.75 V, 0.08 nA. The unit cell dimensions are $a = (1.48 \pm 0.03)$ nm and $b = (1.31 \pm 0.03)$ nm and the interior angles are $(68 \pm 1)°$ and $(112 \pm 1)°$. The packing density is (0.56 ± 0.02) Å^2. ((d)-(f)) 0.80 ML, +0.75 V, 0.1 nA. Unit cell dimensions: $c = (2.89 \pm 0.03)$ nm and $d = (1.50 \pm 0.03)$ nm. Interior angles: $(60 \pm 1)°$ and $(120 \pm 1)°$. Packing density: (0.53 ± 0.01) Å^2. ((g)-(i)) 0.98 ML, +0.75 V, 0.05 nA. Unit cell dimensions: $e = (1.86 \pm 0.03)$ nm, $f = (2.72 \pm 0.03)$ nm. Interior angles: $(43 \pm 1)°$ and $(137 \pm 1)°$. Packing density: (0.58 ± 0.01) Å^2. ((j)-(l)) 1.00 ML, +0.75 V, 0.08 nA. Unit cell dimensions: $g = (1.32 \pm 0.03)$ nm, $h = (1.30 \pm 0.03)$ nm. Interior angles: $(88 \pm 1)°$ and $(92 \pm 1)°$. Packing density: (0.58 ± 0.02) Å^2. The contrast was enhanced in the right-hand sides of the STM images in (a), (d), and (g) by application of a different color scale to render the different types of symmetry reduction more clearly visible.

2. X-ray photoelectron spectroscopy and x-ray absorption spectroscopy

The black spectrum in Fig. 5 is the C 1s XP spectrum of a monolayer (±0.1 ML) of FePc on Cu(111) prepared by room-temperature deposition. The line has two main components, both of which are broadened towards higher binding energy. The most intense feature at around 284.2 eV is due to photoemission from the 24 carbon atoms of the benzo groups. The second component at around 285.4 eV is due to photoemission from the eight carbon atoms which are bonded to the pyrrole nitrogen atoms. In addition, shake-up features at around 1.9 eV higher binding energy than that of the main lines are expected,[28,29] but are here largely suppressed due to the interaction of the FePc with the metallic Cu(111) surface. The broadening of the two main peaks, which is particularly pronounced for the benzo-related peak, is assigned to a combination of out-of-plane deformation of the Pc macrocycle and uneven charge distribution over the two molecular axes.[27]

Fig. 6(a) contains, as black curve, the N 1s XP spectrum of the room temperature preparation. The first moment of the intensity is located at 398.67 eV, and its width is approximately 1 eV. In comparison to the N 1s lines of a FePc multilayer and FePc monolayers on more inert surfaces,[30–32] the peak is broadened due to the increased chemical difference of the bridging aza (N_{aza}) and pyrrole (N_{pyr}) nitrogen atoms as a result of charge transfer from the Cu(111) surface to the adsorbates.[27]

Finally, the spectra in black color in Fig. 7 are the N 1s x-ray absorption (XA) spectra of the monolayer prepared at room temperature in normal and grazing x-ray incidences on the sample. The spectra are normalized to the intensity of the step edge related to the vacuum level, measured at about 25 eV above the adsorption threshold (Fig. S2 in the supplementary material[25]). The angle dependence of the π^* resonances confirms the flat geometry of FePc on the Cu(111) surface. The low-lying π^* resonance at 398-399 eV contains two distinguishable features, which are related to the N_{pyr} and N_{aza} nitrogen atoms. In XA spectra of FePc multilayers[30]

and FePc monolayers on inert surfaces such as Au(111)[31] or HOPG,[32] these two features are not as clearly resolved. The observation that the two peaks are more easily identified for FePc/Cu(111) is partly a result of their larger separation as compared to what is found for pristine FePc and FePc adsorbed on more inert surfaces[27] and partly of charge transfer from the Cu(111) support to the adsorbates. More charge is transferred to the N_{aza} than to the N_{pyr} atoms,[27] which leads to a reduction of the N_{aza}-related LUMO intensity in comparison to the N_{pyr} intensity. Similar observations have been made for the adsorption of CoPc on the Cu(111)[33] and FePc on the Ag(111) surface.[34] In the spectra in Fig. 7, additional π^* resonances are found at higher photon energies, although in particular the region in the range between approximately 399 and 401 eV photon energy is much less well defined than that of the case for FePc multilayers and FePc layers on inert surfaces. Such differences are quite expected in view of the rather strong interaction of the macrocycle part of the FePc adsorbates with the Cu(111) surface and concomitant hybridization of adsorbate and Cu(111) states.[27]

B. Temperature-induced structural changes

1. Scanning tunneling microscopy

Fig. 3 shows the effect of annealing to 250 and 300 °C on the structure of the molecular overlayer. Annealing of a nearly complete FePc monolayer on Cu(111) to 250 °C leads to the formation of large, ordered domains featuring an increased packing density with two distinct molecular orientations. The appearance of the FePc adsorbates is consistent with the data before annealing shown in Fig. 2, and a unit cell can be identified featuring a molecular arrangement as shown in Fig. 3(c). The parameters of this unit cell are given in the figure caption. No major change is observed after annealing the nearly complete monolayer at 270 °C for 30 min. Annealing to 300 °C at 25 min leads to a pronounced reduction of order reflected in a variety of intermolecular arrangements, as is visible from Fig. 3(d). In this figure, red and white arrows indicate examples of locations at which adsorbates have and have not reacted which each other, respectively, as further discussed below.

The effect of annealing on a submonolayer is similar to that for a monolayer as is illustrated by the STM images in Figs. 3(e) and 3(f). Upon annealing to 300 to 320 °C for 10 min, i.e., at a temperature similar to the onset of sublimation of the FePc solid, the adsorbates re-organize. A portion of the adsorbates are still found to be isolated. These individual adsorbates are oriented with one molecular axis aligned with a close-packed row. Some of them are perfectly aligned, but another fraction deviates from this orientation by up to 9° (cf. Fig. 4(a)). This observation contrasts with the behavior of adsorbates in an as-deposited room temperature submonolayer (up to 0.5 ML), in which the adsorbates predominantly align perfectly with the close-packed rows. Further, a large fraction of the adsorbates arrange in dendrite-like chains. For the adsorbates in such chains the orientation is governed by the intermolecular rather than the adsorbate-surface interaction.

In addition to the STM images in Figures 1 and 2, we also report dI/dV maps at different biases of individual adsorbates after annealing to 320 °C in Fig. 4. In these dI/dV maps, the same kind of symmetry reduction is seen as in STM images of the room temperature preparations. Indeed, the symmetry reduction is even clearer in the dI/dV maps in comparison to the STM images, and also a switching of contrast between the two molecular axes with bias is observed.

2. X-ray photoelectron spectroscopy and x-ray absorption spectroscopy

The orange line in Fig. 5 is the C 1s spectrum of a monolayer of FePc on Cu(111) after annealing of the surface to 320 °C. In comparison to the black room temperature spectrum in the same figure, the general lineshape with the presence of the benzo and pyrrole peaks is preserved; at the same time, a quite significant broadening of the benzo-related peak is observed together with a shift of the pyrrole-related peak to a higher binding energy. In addition, a new, small low binding-energy shoulder emerges at around 283.4 eV binding energy. The full width at half-maximum (FWHM) of the benzo

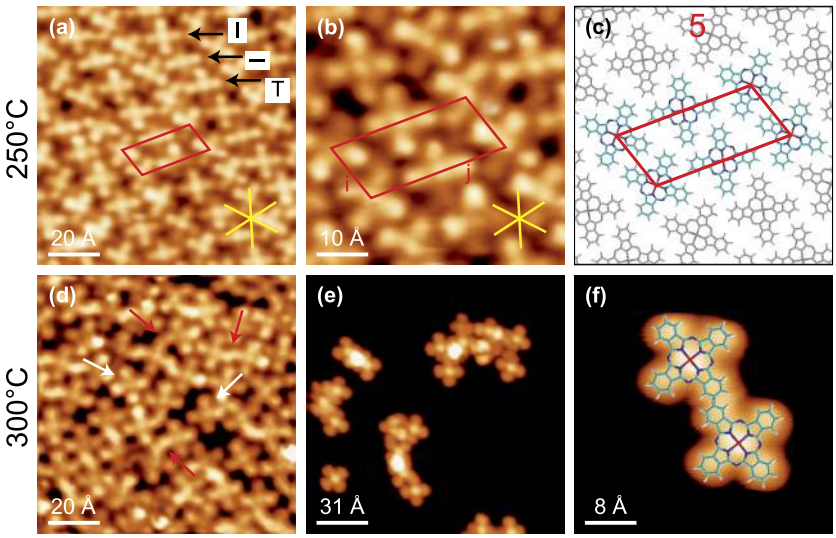

FIG. 3. Effect of annealing on the FePc/Cu(111) layer. ((a)-(c)) Annealing temperature 250°C, ((d)-(f)) 300°C. (a) +0.75 V, 0.05 nA, 100×100 Å^2. The type of symmetry breaking is indicated by letters. (b) +0.75 V, 0.05 nA, 50×50 Å^2. The red tetragon shows the unit cell of the molecular assembly. (c) Sketch of the molecular assembly of the structure obtained by annealing to 250°C. Cell parameters: $i = (1.25 \pm 0.03)$ nm, $j = (2.78 \pm 0.03)$ nm, interior angles $(72 \pm 1)°$ and $(108 \pm 1)°$. (d) +0.75 V, 0.10 nA, 100 ×100 Å^2. Red arrows indicate the formation of C–C bonds in a homocoupling reaction, while the white arrows indicate molecules where such a reaction has not taken place. (e) −0.80 V, 0.10 nA, 155×155 Å^2. (f) 0.50 V, 0.10 nA, 40×40 Å^2.

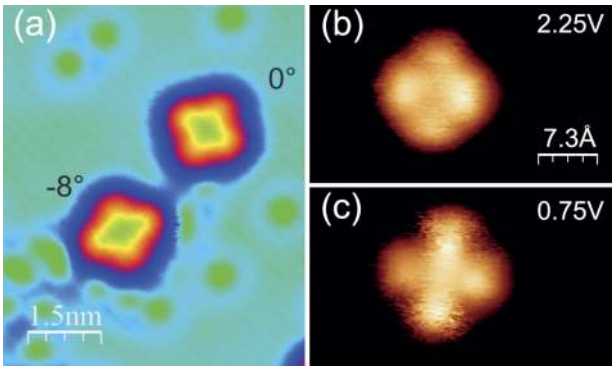

FIG. 4. STM image and dI/dV maps of FePc/Cu(111) after annealing to 320°C. (a) Two orientations of the adsorbates are induced: one with a molecular axis aligned with a close-packed surface direction and one deviating from that direction by −8° (0.9 V, 0.25 nA). ((b) and (c)) Constant height dI/dV maps of a single FePc molecule on Cu(111). The bias is indicated. A switch-over of the contrast is observed upon changing the bias.

peak changes from 0.64 eV to 0.80 eV. As will be detailed and motivated in Sec. IV, the spectrum can be further analyzed by assuming contributions of new species. One of these contributions results from newly created intermolecular C–C bonds and is found at around 0.3 eV higher binding energy than the benzo-related peak.[35] The simultaneously observed broadening of the low-binding energy flank is attributed to changes in the bonding of the FePc molecules to the surface after annealing.

Fig. 6(a) shows the N 1s XP spectra of both the non-annealed (black) and annealed (orange) monolayers of FePc/Cu(111). Fig. 6(b) reproduces the evolution of the N 1s line during annealing in the form of a series of TD-XPS measurements. Prior to annealing, the N 1s peak, with a first moment at 398.67 eV, contains components due to two chemically different nitrogen atoms (N_{pyr} and N_{aza}), which normally cannot be resolved.[27,36] The somewhat asymmetric shape of the line towards lower binding energy can be ascribed to an asymmetric charge redistribution in the molecule upon adsorption on the Cu(111) surface.[27]

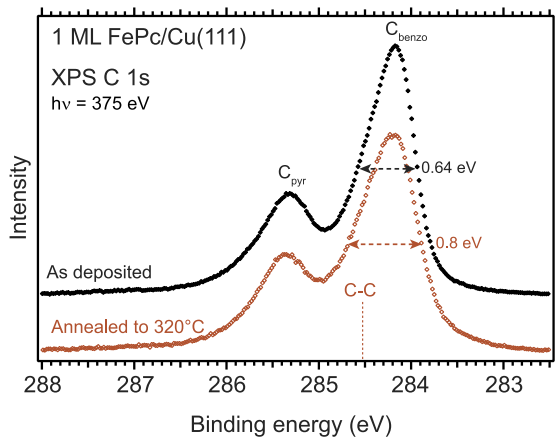

FIG. 5. C 1s XP spectra of the 1 ML film of FePc/Cu(111). A comparison of the spectra before (black) and after annealing to 320°C (orange), with both spectra recorded at room temperature, show the increase in FWHM from 0.64 eV to 0.80 eV. The homocoupling reaction of the FePc adsorbates results in the formation of C–C bonds, which have a characteristic binding energy at the indicated position. Both spectra were acquired at room temperature.

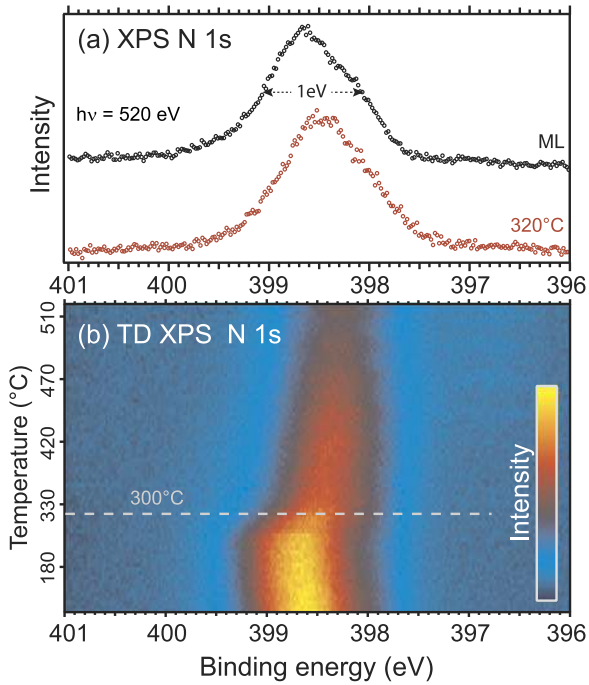

FIG. 6. N 1s XP spectra of 1 ML FePc/Cu(111). The layer was prepared at room temperature and subsequently annealed. (a) Comparison of the N 1s spectrum of the room temperature preparation (black) to that of the monolayer annealed to 320°C (orange). Both spectra were acquired at room temperature and normalized to their area after background removal. (b) N 1s TD-XPS experiments performed in the temperature range between 31°C –520°C. The color scale represents the raw intensity as measured.

Upon annealing, the N 1s line is shifted to lower binding energy by −0.15 eV to 398.52 eV. A similar, but a bit smaller shift of around −0.10 eV is also found for the main line in the Fe 2p spectrum (Fig. S3 in the supplementary material[25]). A direct comparison of the N 1s lineshape before and after annealing shows that it is virtually unchanged (Fig. S4 in the supplementary material[25]) and thus not further affected by the shift. The N 1s shift with annealing is also clearly visible in the temperature dependent XP (TD-XP) spectra in Fig. 6(b). Also visible is an attenuation of the N 1s intensity with temperature, which starts at slightly below 300 °C. Since the STM results do not suggest any drastic modification of the inner parts of the macrocycle with temperature, the signal attenuation is attributed to desorption of adsorbates at these temperatures.

Figure 7 compares the π^* region of the N 1s XA spectra before and after annealing. The N 1s XA spectrum measured on the FePc/Cu(111) layer annealed to 320 °C differs from the spectrum acquired on the non-annealed surface primarily in the shape of the lowest π^* resonance, which contains resonance contributions of the N_{aza} and N_{pyr} atoms. The angular dependence is unchanged, which shows that the planar geometry of the molecules on the surface is preserved. What is changed is the location of the resonance, which for the room temperature samples is found at 398-399 eV: the resonance is shifted to lower energy, quite as expected on the basis of the N 1s XPS results. Moreover, the distinction between the two features related to the N_{aza} and N_{pyr} atoms is less clear in comparison to the spectrum obtained before annealing, and

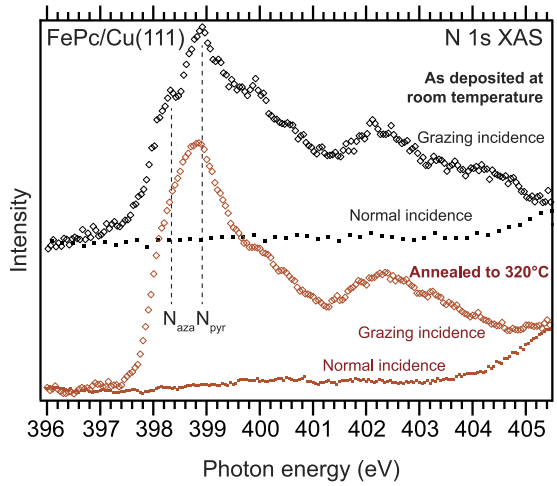

FIG. 7. Comparison of the N 1s XA spectra of 1 ML FePc/Cu(111) before (black) and after annealing to 320 °C (orange). Both spectra were measured at room temperature. The measurements were taken in normal and grazing (70° from the surface normal) incidences of the x-ray beam on the sample.

the spectral intensity at around 400 eV on the high photon energy side of the lowest resonance is reduced.

IV. DISCUSSION

A. Symmetry reduction

The apparent symmetry reduction of FePc adsorbates on Cu(111), observed in STM images, has been reported before.[23,27] For adsorbates in close-packed islands at 0.5 ML coverage, it has been attributed to the formation of anionic FePc with an uptake of charge density from the surface and its inequivalent distribution over the two molecular axes in combination with a distortion of the macrocycle skeleton.[27] The somewhat peculiar switch-over in contrast between isolated molecules and those in close-packed islands, where the bright axis is oriented along the close-packed surface direction in the latter and perpendicularly to this direction in the former,[23] has previously been associated with a mixture of molecular orbitals produced by the molecule-metal interaction.[37]

It seems likely that the occurrence of other types of symmetry reduction (L- and T-type of adsorbates in Fig. 2) than the twofold one (I-type of adsorbates) at a coverage of 0.98 ML also is attributable to a combination of charge transfer from the surface to the adsorbates, rehybridization of the adsorbate with the surface electronic states, and bending of the molecular framework of the adsorbates. Since the twofold symmetry reduction of isolated FePc adsorbates at low coverage has a mixed electronic/geometric character,[27] the symmetry breaking at close-to monolayer coverage is also expected to have such a mixed nature. There exists a difference, though, in that the twofold symmetry reduction and concomitant charge transfer from the Cu(111) surface to the adsorbates only require a breakup of the frontier orbital degeneracy. In contrast, the other types of symmetry reduction necessitate a more complex rehybridization of the molecular orbitals. This suggests that the binding sites of the molecules and their surface registry have changed at least slightly at a coverage of 0.98 ML in comparison to lower coverage. Therefore, it also seems likely that the FePc overlayer at higher coverage is not commensurate with the Cu(111) surface and that, therefore, not all FePc adsorbates have the same binding site. Finally, we note that annealing of the FePc layer on Cu(111) does not remove the mechanism for symmetry breaking, as is illustrated by the STM image and dI/dV maps in Fig. 4. The changing appearance of the dI/dV map with bias underlines the orbital selectivity and thus partially electronic character of the symmetry breaking effect.[27]

B. Temperature-induced structural changes

An inspection of the N 1s TD-XP spectra in Fig. 6(b) shows that while annealing to 250 °C leaves the N 1s intensity unchanged and hence does not lead to any desorption of FePc adsorbates from the Cu(111) surface [cf. the STM images in Figs. 3(a) and 3(b)], annealing to 320 °C reduces the intensity to approximately 75% of the initial value and thus implies desorption of around 25% of the FePc from the surface. In addition, for the annealed FePc overlayers, another trend can be observed in the STM images: A large fraction of the molecules, 82% in the series of image from which Fig. 3(d) was taken, form dendritic chains and clusters upon annealing. In these structures, the FePc molecules come significantly closer to each other than what the van der Waals radii of the atoms would suggest is possible. This indicates dehydrogenation and polymerization of the molecules in a homocoupling reaction[18] and, indeed, thermally induced dehydrogenation and polymerization of phthalocyanine molecules have been reported previously for the Ag(111) surface.[16] We note that any appreciable dissociation beyond dehydrogenation is not discernible from the STM images (cf. Fig. 3).

Upon annealing to 320 °C the N 1s peak in the XP spectrum in Fig. 6 shifts by 0.15 eV to lower binding energy, while the lineshape is unchanged. In contrast, annealing leads to more complex modification of the C 1s line, as can been seen from the spectra in Fig. 5: in comparison to the spectrum of the as-prepared FePc/Cu(111) layer, a broadening is observed on both the low and high binding energy sides of the benzo-related peak located at around 284.5 eV in the spectrum of the FePc/Cu(111) layer annealed to 320 °C.

It is tempting to ascribe the N 1s downshift to the effects of the homocoupling reaction, since a similar shift has been observed both in the N 1s and C 1s XP spectra of homocoupled porphine molecules on a Ag(111) surface.[18] However, as reported above in the discussion of the STM images, even after annealing to 300 °C, a large fraction of the adsorbates on the order of 15%–20% remain isolated and do not undergo any intermolecular reaction. If the downshift in the N 1s XP spectrum had been due to the reaction, the lineshape should have changed, since there would be contributions of adsorbates that have reacted and those that have not. This is not the case, and therefore it seems more probable that the shift of the N 1s peak has a different explanation. Indeed, with regard to the N 1s binding energy, the case of porphine homocoupling can be expected to be quite different from that of phthalocyanine homocoupling, since the hetero-nitrogen atoms in porphine

are much closer to the homocoupling reaction site at the outer perimeter of the molecule than in phthalocyanine.

A possible alternative explanation for the N 1s downshift is a closer distance between surface and adsorbate, given rise to by a stronger adsorbate-surface interaction. Such a closer distance would lead to a more efficient screening of the core hole. Assuming only polarization screening, the downshift relative to the binding energy of the N 1s line of the non-annealed sample is given by $\Delta E_{BE} = -(e^2/4\pi\epsilon_0)(1/r_{non-annealed} - 1/r_{annealed})$, where $r_{non-annealed}$ and $r_{annealed}$ are the distances between the FePc adsorbates in the non-annealed and those in the annealed case, respectively, to their image charges in the Cu(111) surface. Using a distance between FePc adsorbate and image plane of 2.69 Å in the room temperature monolayer determined in previous x-ray standing wave experiments[38] and assuming that the distance between the core hole and its image charge is double this distance, one obtains a difference in height of the FePc adsorbate over the surface in the non-annealed and the annealed layer of 0.14 Å.

It should be noted, though, that it is likely that the stronger adsorbate-surface interaction, instead of only providing a more efficient polarization screening of the core hole, leads to a more efficient charge transfer screening pattern. Although such a pattern implies a different value for the change in adsorbate-surface distance, the argumentation is rather the same: more efficient core-hole screening due to a decreased adsorbate-surface distance leads to a lower binding energy. Thus, the result of a shorter bonding distance is still valid.

Another alternative reason for the N 1s shift could be that annealing might induce an increased ground state charge transfer from the Cu(111) support to the adsorbates. Such a charge transfer would be expected to affect both the N 1s and C 1s binding energies. However, the rather unchanged π^* lineshape in the N 1s XA spectrum in Fig. 7 does not lend support to the assumption of an increased ground state charge transfer and we therefore disregard it.

As already stated, the C 1s line in Fig. 5 does not follow the same trend of a rigid downshift in binding energy. Instead, a broadening towards both edges of the benzo-related peak is found. The observation can be explained from a combination of the effects of a smaller surface-adsorbate distance with those of a homocoupling reaction, in which one or two hydrogen atoms are removed from the benzo moieties involved in the reaction of neighboring molecules. The hydrogen atoms freed in the homocoupling reaction probably form dihydrogen gas, since hydrogen desorbs from the Cu(111) surface at around room temperature,[39] and the C–H bonds are replaced by C–C bonds. According to Minkov *et al.*,[35] the C 1s binding energy of the carbons atoms linking together the phenyl rings in biphenyl is 0.20–0.36 eV higher than that of the other phenyl carbon atoms. A similar binding energy shift should be applicable to the carbon atoms in the C–C bonds formed in the homocoupling reaction, which would explain the broadening of the high binding energy side of the benzo peak in the C 1s spectrum. At the same time, the carbon atoms on the benzo moiety are affected by the reduced surface-adsorbate distance in the same way as the nitrogen atoms, and thus a downshift in agreement with that in the N 1s XP spectra is to be expected. Hence, the broadening on the low-binding energy side of the benzo peak is due to the changed distance between Cu(111) surface and FePc adsorbates. Altogether, a combination of effects can explain the broadening on both flanks of the benzo peak in the C 1s spectrum.

At the same time, also a slight upshift upon annealing of the pyrrole-related peak at around 285.3 eV is observed, although a downshift would be expected in accordance with that of the N 1s peak. However, this upward shift is attributable to the broadening of the benzo peak rather than a real shift, since the broadening benzo peak provides an additional sloping background to the pyrrole peak. A curve fitting or theoretical analysis could give proper input to the question of the location and shift of the pyrrole peak; since curve fitting of the rather complex lineshape would require rather detailed input on the number and intensities of the components of the benzo peak, we refrain from it here, though.

A shortening of the distance of both the isolated and homocoupled FePc adsorbates from the Cu(111) upon annealing to 320 °C implies that the molecule initially, when prepared at room temperature, is in a different state than after annealing. Already this room temperature state is of a chemisorptive nature and can be viewed as a chemisorbed π-bonded precursor state. We suggest that annealing leads to a weakening of the intramolecular bonds and a breaking-up of the π-bonds, which is accompanied by a strengthening of the surface bond due to a switch-over to σ-bonding. The adsorbate is thus transferred to a second, more strongly bonded chemisorption state. The same kind of scheme is known to occur under a certain condition for smaller double- and triple-bonded molecules at transition metal surfaces and has, e.g., been observed for ethene on a stepped Cu(410) surface.[40] It has not been observed previously for a double-bonded hydrocarbon on a flat Cu(111) surface, though,[41] the reason presumably being that the barrier towards the second chemisorption state is too unfavorable. Here, we find spectroscopic evidence for a transfer of the FePc adsorbates into such a second chemisorptive state by annealing, possibly as a result of a changed barrier to desorption. The fact that the intramolecular bonds in this state indeed are weakened is supported by additional experiments in which we have observed that exposure of the annealed surface to atomic oxygen leads to further decomposition of the FePc adsorbates, while this is not the case for the as-prepared room temperature surface. An interesting consequence of this change in reactivity might be that the annealed Cu-supported macrocycles also might be more susceptible to acting as a catalyst.

V. CONCLUSIONS

We have systematically studied the formation of a molecular monolayer of FePc on Cu(111) from submono- to mono-layer coverages and the occurring FePc adsorption geometries. Common to all coverages is that the molecules lie flat on the Cu(111) surface. Common for all coverages is also that, in STM, a symmetry reduction of the appearance of the FePc adsorbates has been observed, even in those cases in which the molecules do not align with their molecular

axes along the crystallographic directions of the (111) lattice anymore. Moreover, at sufficiently high submonolayer coverage, not all FePc adsorbates have a twofold symmetric appearance (rather than the fourfold symmetric appearance expected from the gas phase structure of the molecule), but also different types of onefold symmetry are observed. This suggests a rather complex mechanism of symmetry breaking, with rehybridization of the molecular states with support states, charge donation from the metallic surface to the adsorbate, and out-of-plane distortion of the macrocycle skeleton of the molecule contributing. We have also shown that symmetry reduction persists after annealing of the molecules.

Annealing of a monolayer of FePc/Cu(111), prepared at room temperature, leads initially to a re-ordering of the molecular overlayer and at higher temperature (320 °C) to partial desorption. The remaining adsorbates bind more strongly to the Cu(111) surface, as can be observed from the XP and XA spectra. We have explained the shortened surface-adsorbate distance in terms of a rehybridization of the molecular states and a switch-over from surface π to σ binding. This change could explain a significantly changed reactivity of the FePc adsorbates.

Further, annealing also leads to partial dehydrogenation and polymerization of the benzo groups of a large fraction of the adsorbates. This effect is visible not only in high-resolution STM images, but also as change of lineshape of the C 1s core level spectrum. As a perspective, a formation of FePc dendrite-like chains on Cu(111) surface at submonolayer coverage upon annealing could help in producing stable single molecule nanowires.

ACKNOWLEDGMENTS

We would like to thank Luke Rochford for providing us with the purified FePc for the STM experiments. The staff at the MAX IV Laboratory and beamline I311 are acknowledged for their assistance during the spectroscopy experiments. We would like to acknowledge our funding sources Vetenskapsrådet (Grant No. 2010-5080), the European Commission via the Marie Curie Initial Training Network SMALL (Grant No. 238804), the European Research Council via the ERC Advanced Grant MolArt (Grant No. 247299), the Munich Center for Advanced Photonics (MAP), and the Technische Universität München–Institute for Advanced Study, funded by the German Excellence Initiative. A.W. was supported by the International Max Planck Research School of Advanced Photon Science and W.A. acknowledges funding by the German Research Foundation (DFG) via a Heisenberg professorship.

[1]C. Wäckerlin, D. Chylarecka, A. Kleibert, K. Müller, C. Iacovita, F. Nolting, T. A. Jung, and N. Ballav, Nat. Commun. **1**, 61 (2010).
[2]C. Isvoranu, B. Wang, K. Schulte, E. Ataman, J. Knudsen, J. N. Andersen, M.-L. Bocquet, and J. Schnadt, J. Phys.: Condens. Matter **22**, 472002 (2010).
[3]P. Liljeroth, J. Repp, and G. Meyer, Science **317**, 1203 (2007).
[4]Y. Okawa, S. K. Mandal, C. Hu, Y. Tateyama, S. Goedecker, S. Tsukamoto, T. Hasegawa, J. K. Gimzewski, and M. Aono, J. Am. Chem. Soc. **133**, 8227 (2011).
[5]Y. L. Huang, Y. H. Lu, T. C. Niu, H. Huang, S. Kera, N. Ueno, A. T. S. Wee, and W. Chen, Small **8**, 1423 (2012).
[6]P. Borghetti, A. El-Sayed, E. Goiri, C. Rogero, J. Lobo-Checa, L. Floreano, J. E. Ortega, and D. G. de Oteyza, ACS Nano **8**, 12786 (2014).
[7]M. Schmid, A. Kaftan, H.-P. Steinrück, and J. M. Gottfried, Surf. Sci. **606**, 945 (2012).
[8]M. Toader, P. Shukrynau, M. Knupfer, D. R. T. Zahn, and M. Hietschold, Langmuir **28**, 13325 (2012).
[9]A. Ruocco, F. Evangelista, R. Gotter, A. Attili, and G. Stefani, J. Phys. Chem. C **112**, 2016 (2008).
[10]A. Zhao, Q. Li, L. Chen, H. Xiang, W. Wang, S. Pan, B. Wang, X. Xiao, J. Yang, J. G. Hou, and Q. Zhu, Science **309**, 1542 (2005).
[11]N. Tsukahara, K. Noto, M. Ohara, S. Shiraki, N. Takagi, Y. Takata, J. Miyawaki, M. Taguchi, A. Chainani, S. Shin, and M. Kawai, Phys. Rev. Lett. **102**, 167203 (2009).
[12]T. Niu, M. Zhou, J. Zhang, Y. Feng, and W. Chen, J. Phys. Chem. C **117**, 1013 (2013).
[13]Y. Bai, F. Buchner, M. T. Wendal, I. Kellner, A. Bayer, H.-P. Steinrück, H. Marbach, and J. M. Gottfried, J. Phys. Chem. C **112**, 6087 (2008).
[14]J. Åhlund, J. Schnadt, K. Nilson, E. Göthelid, J. Schiessling, F. Besenbacher, N. Mårtensson, and C. Puglia, Surf. Sci. **601**, 3661 (2007).
[15]B. Stadtmüuller, I. Kröger, F. Reinert, and C. Kumpf, Phys. Rev. B **83**, 085416 (2011).
[16]K. Manandhar, T. Ellis, K. T. Park, T. Cai, Z. Song, and J. Hrbek, Surf. Sci. **601**, 3623 (2007).
[17]K. Manandhar, K. T. Park, S. Ma, and J. Hrbek, Surf. Sci. **603**, 636 (2009).
[18]A. Wiengarten, K. Seufert, W. Auwärter, D. Ecija, K. Diller, F. Allegretti, F. Bischoff, S. Fischer, D. A. Duncan, A. C. Papageorgiou, F. Klappenberger, R. G. Acres, T. H. Ngo, and J. V. Barth, J. Am. Chem. Soc. **136**, 9346 (2014).
[19]R. Lindner and A. Kühnle, ChemPhysChem **16**, 1582 (2015).
[20]R. Nyholm, J. N. Andersen, U. Johansson, B. N. Jensen, and I. Lindau, Nucl. Instrum. Methods Phys. Res., Sect. A **467-468**, 520 (2001).
[21]I. Horcas, R. Fernández, J. M. Gómez-Rodrígues, J. Colchero, J. Gómez-Herrero, and A. M. Baro, Rev. Sci. Instrum. **78**, 013705 (2007).
[22]L. A. Rochford, I. Hancox, and T. S. Jones, Surf. Sci. **628**, 62 (2014).
[23]S.-H. Chang, S. Kuck, J. Brede, L. Lichtenstein, G. Hoffmann, and R. Wiesendanger, Phys. Rev. B **78**, 233409 (2008).
[24]A. Scarfato, S.-H. Chang, S. Kuck, J. Brede, G. Hoffmann, and R. Wiesendanger, Surf. Sci. **602**, 677 (2008).
[25]See supplementary material at http://dx.doi.org/10.1063/1.4942121 for STM images of FePc/carbon monoxide co-adsorption experiments for determination of the FePc binding site on Cu(111), N 1s XAS data of a FePc monolayer on Cu(111) (as-prepared at room temperature and annealed to 320 °C) over the extended photon energy range of 396 - 420 eV, comparison of the Fe 2p XP spectra of FePc/Cu(111) before and after annealing, and comparison of the N 1s XP spectra of FePc/Cu(111) before and after annealing.
[26]J. C. Buchholz and G. A. Somorjai, J. Chem. Phys. **66**, 573 (1977).
[27]O. Snezhkova, J. Lüder, A. Wiengarten, S. R. Burema, F. Bischoff, Y. He, J. Rusz, J. Knudsen, M.-L. Bocquet, K. Seufert, J. V. Barth, W. Auwärter, B. Brena, and J. Schnadt, Phys. Rev. B **92**, 075428 (2015).
[28]B. Brena and Y. Luo, Radiat. Phys. Chem. **75**, 1578 (2006).
[29]B. Brena, Y. Luo, M. Nyberg, S. Carniato, K. Nilson, Y. Alfredsson, J. Åhlund, N. Mårtensson, H. Siegbahn, and C. Puglia, Phys. Rev. B **70**, 195214 (2004).
[30]C. Isvoranu, J. Knudsen, E. Ataman, K. Schulte, B. Wang, M.-L. Bocquet, J. N. Andersen, and J. Schnadt, J. Chem. Phys. **134**, 114711 (2011).
[31]C. Isvoranu, B. Wang, E. Ataman, K. Schulte, J. Knudsen, J. N. Andersen, M.-L. Bocquet, and J. Schnadt, J. Phys. Chem. C **115**, 20201 (2011).
[32]C. Isvoranu, J. Åhlund, B. Wang, E. Ataman, N. Mårtensson, C. Puglia, J. N. Andersen, M.-L. Bocquet, and J. Schnadt, J. Chem. Phys. **131**, 214709 (2009).
[33]E. Annese, J. Fujii, I. Vobornik, and G. Rossi, J. Phys. Chem. C **115**, 17409 (2011).
[34]F. Petraki, H. Peisert, U. Aygül, F. Latteyer, J. Uihlein, A. Vollmer, and T. Chassé, J. Phys. Chem. C **116**, 11110 (2012).
[35]I. Minkov, F. Gel'mukhanov, H. Ågren, R. Friedlein, C. Suess, and W. R. Salaneck, J. Phys. Chem. A **109**, 1330 (2005).
[36]J. Åhlund, K. Nilson, J. Schiessling, L. Kjeldgaard, S. Berner, N. Mårtensson, C. Puglia, B. Brena, M. Nyberg, and Y. Luo, J. Chem. Phys. **125**, 034709 (2006).
[37]B. W. Heinrich, C. Iacovita, T. Brumme, D.-J. Choi, L. Limot, M. V. Rastei, W. A. Hofer, J. Kortus, and J.-P. Bucher, J. Phys. Chem. Lett. **1**, 1517 (2010).
[38]I. Kröger, B. Stadtmüller, C. Kleimann, P. Rajput, and C. Kumpf, Phys. Rev. B **83**, 195414 (2011).
[39]K. Mudiyanselage, Y. Yang, F. M. Hoffmann, O. J. Furlong, J. Hrbek, M. G. White, P. Liu, and D. J. Stacchiola, J. Chem. Phys. **139**, 044712 (2013).
[40]T. Kravchuk, V. Venugopal, L. Vattuone, L. Burkholder, W. T. Tysoe, M. Smerieri, and M. Rocca, J. Phys. Chem. C **113**, 20881 (2009).
[41]M. Witko and K. Hermann, Appl. Catal., A **172**, 85 (1998).